Analytical Methods

Accepted Manuscript

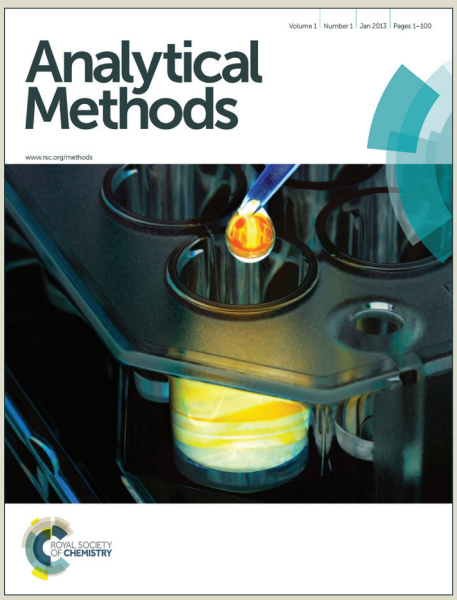

ROYAL SOCIETY OF CHEMISTRY

www.rsc.org/methods

Analytical Methods

RSCPublishing

ARTICLE

Nanoscaled Au-Horseradish Peroxidase Composite Fabricated by an Interface Reaction and Its Characterization, Immobilization and Biosensing

Cite this: DOI: 10.1039/x0xx00000x

Received ooth,
Accepted ooth

DOI: 10.1039/x0xx00000x

www.rsc.org/

Suli Liu,[a] Tianxiang Wei,[a] Qian Liu,[a] Wenwen Tu,[a] Yaqian Lan,[a] Min Han,[a] Jianchun Bao,*[a] Zhihui Dai*[a]

[a]Jiangsu Collaborative Innovation Center of Biomedical Functional Materials and Jiangsu Key Laboratory of Biofunctional Materials, School of Chemistry and Materials Science, Nanjing Normal University, Nanjing, 210023, P. R. China

*Corresponding author: daizhihuii@njnu.edu.cn; baojianchun@njnu.edu.cn

We develop a novel strategy for the biosensing application of hydrogen peroxide (H_2O_2) using nanoscaled Au-horseradish peroxidase (HRP) composite thin film synthesized by liquid-liquid interface reaction. Through the interaction between Au nanoparticles and NH_2-terminated HRP, HRP is effectively combined with Au in the thin film. The nanocomposite membrane is extracted on the surface of ITO electrode directly, retaining its bioactivity during the immobilization process, which can detect the substrate in situ. The immobilized HRP displays an excellent electrocatalytical response to the reduction of H_2O_2, with a fast amperometric response (within 5 s), wide linear range (7.9 μM to 3.6 mM), low detection limit (0.035 μM), and a good affinity (K_m^{app} = 0.14 mM) to H_2O_2. The prepared biosensor also exhibits high sensitivity, good reproducibility and long-term stability. Furthermore, it can be successfully exploited for the determination of H_2O_2 released from living cells directly adhered on the modified electrode surface.

1. Introduction

Electrochemical biosensors have been recently applied to many fields including food analysis, biological analysis, environmental monitoring, and medical detection due to their intrinsic advantages such as high sensitivity, portability, relatively low cost, online detection, rapid response, and reusability.[1-2] During the fabrication of biosensors, the strategy for immobilizing the active biomolecules is considered to be one of the crucial aspects, because biomolecules can be easily inactivated or released from the electrodes if they are not properly immobilized. Compared with the conventional immobilization methods of biomolecules,[3-13] such as physical adsorption,[3-6] entrapment,[7] cross-linking,[8-10] covalent binding[11-13] and interface method[14-16], liquid-liquid interface method is attractive owing to its inherent simplicity and low cost. Furthermore, it is an important means to generate self-assemblies of nanocrystals, providing a constrained environment for immobilization of biomolecules.[17,18]

Gold nanoparticles (AuNPs) are one of the most useful metals which have been widely used in many sensing applications in recent years.[19,20] AuNPs have the ability to enhance the electrode conductivity and facilitate the electron transfer. Especially, the small size and biocompatible ability of AuNPs were widely utilized as a base in construction of various biosensors to promote the electron transfer of many proteins, such as horseradish peroxidase (HRP),[21-23] hemoglobin,[24] myoglobin,[25] glucose oxidase[26,27] and superoxide dismutase.[28,29] In this work, we first use the liquid-liquid interface reaction to prepare Au-HRP composite thin film for enzyme immobilization.

Macrophages (i.e. raw 264.7) are known to play an important role in host protection against a wide range of tumors and

microorganisms. Being the first cells to participate in the immunological response, macrophages contribute to their role in host defense by phagocytosis, antigen presentation and the production of cytokines, reactive oxygen species (ROS) and reactive nitrogen species (RNS) involved in the destruction of pathogens.[30] The main ROS and RNS produced in the macrophages are $O_2^{\bullet-}$, hydrogen peroxide (H_2O_2) and nitric oxide (NO).[31,32] However, excess ROS and RNS production have been implicated in many inflammatory diseases.[33-35]

In this work, nanoscaled Au-HRP composite thin film is easily prepared through the interaction between assembly Au NPs and NH_2-terminated HRP at the toluene-water interface. ITO electrode is chosen to extract the thin films up. Based on the ordered Au-HRP nanocomposite, a sensitive H_2O_2 biosensor is constructed. Compared with the conventional immobilization method, the biosensor has good sensitivity, reproducibility and long-term stability. The monitoring of H_2O_2 released from raw 264.7 macrophage cells using the proposed sensor is also demonstrated.

2. Experiments

2.1. Materials and Reagents

HRP (E.C.1.11.1.7, 250 units mg^{-1}) was purchased from Sigma and used as received. H_2O_2 (30 % W/V solution) solution was purchased from Beijing Chemical Reagent (Beijing, China). Indium tin oxide (ITO) glass (1.1 mm thickness, less than 100 Ω resistance) was purchased from Conduc Optics and Electronics Technology. $HAuCl_4$ was purchased from Shanghai Chemical Reagent Co. Cetyltrimethyl ammonium bromide (CTAB) was purchased from Tianjin Chemical Reagent Institute. Hydrazine hydrate was purchased from Shanghai Ling Feng Chemical Reagent Co., Ltd.. Triphenylphosphine (PPh_3) was purchased from Shanghai Ling Feng Chemical Reagent Co., Ltd.. Toluene was purchased from Sinopharm Chemical Reagent Co., Ltd.. Phosphate buffer solutions (PBS, 0.1 M) with various pH values were prepared by mixing stock standard solutions of K_2HPO_4 and KH_2PO_4 and adjusting the pH with H_3PO_4 or NaOH. All other chemicals were of analytical grade and were used without further purification. All solutions were made up with doubly distilled water.

2.2. Apparatus

The morphology and particle sizes of the samples were characterized by field emission scanning electron microscopy (FESEM) (LEO1530 VP) at an acceleration of 15 kV. Energy-dispersive spectroscopy (EDS) was performed on the microscope with a PV9100 scanning electron microanalyzer. UV-vis absorption spectrum was obtained on a Varian Cary 5000 spectrophotometer. Circular dichroic (CD) measurements were made on JASCO Model J-810 dichrograph (Japan Spectroscopic Co. Ltd., Tokyo, Japan) at room temperature in a 1 cm quartz cuvette. Phase characterization was performed by means of X-ray diffraction (XRD) using a D/Max-RA diffractometer with Cu K_α radiation. Cyclic voltammetric and amperometric measurements were performed on CHI 660B electrochemical workstation (CH Instruments, USA). All electrochemical experiments were carried out in a cell containing 5.0 mL 0.1 M PBS at room temperature (20 ± 2 °C) and using a platinum wire as auxiliary, a saturated calomel electrode as a reference and the modified ITO electrode as a working electrode. All solutions were deoxygenated by bubbling highly pure nitrogen for at least 15 min and maintained under nitrogen atmosphere during the measurements. The amperometric experiments were carried out by applying a potential of -0.4 V for H_2O_2 on a stirred cell at room temperature (20 ± 2 °C).

2.3. Preparation of Nanoscaled Au-HRP Composite

First, the AuNPs were prepared by a liquid-liquid interface method according to the previous report.[17] Then, 0.75 mL of 2 mg mL^{-1} fresh HRP was dropped to the system and was uniformly spread onto the interface of the prepared AuNPs. After that, the system was kept at room temperature for 12 h. The HRP was chemisorbed into the prepared AuNPs film by the interaction between AuNPs and NH_2-terminated HRP. Au-HRP thin film was formed in the liquid-liquid interface as shown in Fig. S1.

2.4. Preparation of the Biosensor

A sheet of ITO (3 cm × 0.5 cm) was firstly pretreated according to the literature.[31] It was sonicated with dilute ammonia, absolute ethanol and deionized water for about 5 min, respectively. ITO electrode was used to extract the Au-HRP thin films up to obtain Au-HRP modified ITO electrodes and washed by phosphate buffer solutions (PBS, 0.1 M, pH 7.0) to remove any unbounded enzyme from the electrode surface. After that, Au-HRP modified ITO electrodes were dried in the desiccator. The Au/ITO and HRP/ITO electrodes were also prepared for the control experiments. The area of the working surface was approximately 5 ×5 mm^2. All of the prepared electrodes were stored at 4 °C prior to use.

2.5. Cell Culture

Raw 264.7 macrophage cells were grown at 37 °C in Dulbecco's Modified Eagle Medium (DMEM) supplemented with 10% (v/v) fetal bovine serum (FBS), 100 U mL^{-1} penicillin, and 100 mg mL^{-1} streptomycin in a 5% CO_2 environment. After growing to 90% confluence, the cells were then washed three times with PBS (0.145 M NaCl, 1.9 mM NaH_2PO_4, 8.1 mM K_2HPO_4, pH 7.4) and the cell number was estimated by a hemocytometer.

2.6. H_2O_2 Released from Living Cells

Raw 264.7 macrophage cells were incubated with zymosan (250 μg mL^{-1}) in DMEM complete medium in the presence of nitroblue tetrazolium (NBT). For cell adhesion, 0.5 mL of cells at a concentration of 2×10^5 cells mL^{-1} was directly plated on the modified electrode for the electrochemical experiments. The adhered cells were fixed with 2 % glutaraldehyde for 20 min at room temperature.

3. Results

3.1. Characterization of Au-HRP Nanofilm

X-ray diffraction (XRD) is used to study the nano-structured Au film and Au-HRP composite film on ITO substrates (Fig. 1). The diffraction peaks in the range of 10°<2θ<85° can be indexed as cubic structure Au (111), (200), (220), (311) and (222) (JCPDS card, No. 89-3697). The sharp peaks indicate that product is well crystallized. In addition, some diffraction peaks of the In_2O_3 (JCPDS card, No. 65-3170), marked with asterisks, are also observed, which come from the ITO substrates.

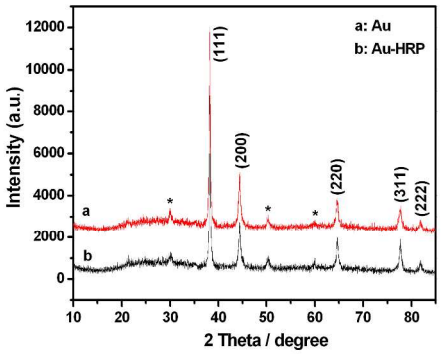

Fig. 1 X-ray diffraction patterns of Au film (a) and Au-HRP composite film (b) on ITO glass substrates.

Figs. 2A and 2B show the FESEM images of the Au nanostructures at low (A) and high (B) magnification on ITO electrodes, respectively. The Au shows chain-like nanostructure which is well distributed. By statistical analysis, the density of AuNPs on ITO plate is about 8×10^{10} atoms cm^{-2}. Fig. 2C shows the FESEM image of the Au-HRP nanocomposite on ITO electrodes. Compared with the case in Fig. 2A, the product is still well distributed, while the chain-like structure trends to aggregate. It results from the formation of the Au-HRP nanocomposite. HRP is immobilized orderly by the interaction between AuNPs and NH_2-terminated HRP. Fig. 2D shows the FTIR spectrum of the AuNPs. The obvious absorption band at 3302 cm^{-1} and 1631 cm^{-1} can be assigned to N-H and O-H vibration arising from amino groups and water absorption, respectively. The broad peak observed around 762 cm^{-1} is attributed to the N-H vibration. Therefore, the results forcefully indicate that the surface modification of amino groups is successful.

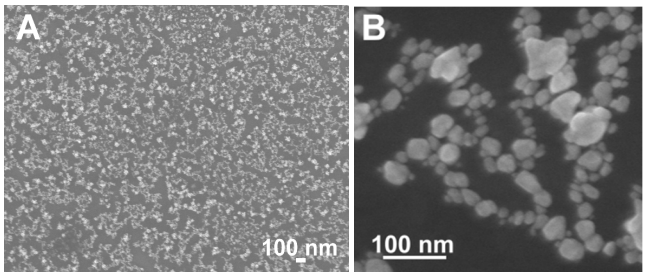

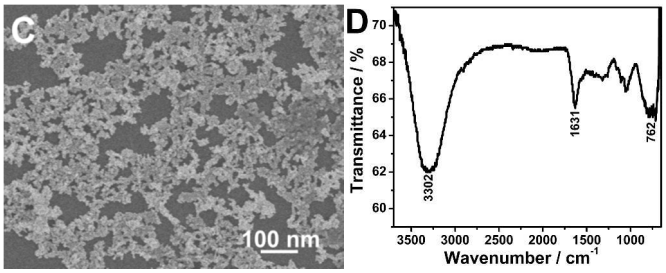

Fig. 2 FESEM images of the Au at low (A) and high (B) magnification and Au-HRP nanocomposite (C) on ITO electrodes. (D) FTIR spectrum of the AuNPs. Au and Au-HRP nanocomposite film are prepared by the liquid-liquid interface reaction.

Fig. 3 shows the UV-vis spectra of Au, HRP and Au-HRP, respectively. Au does not show any absorption peaks (curve a). Comparing the two curves from Au-HRP (curve b) and HRP (curve c), the absorption band of HRP is located at 400 nm which is at the same position as the Au-HRP, suggesting that HRP is immobilized on Au and maintains its native structure. By calculation analysis, the density of HRP on Au is 1 mg mL^{-1}. In other words, such immobilizing process does not destroy the structure of HRP and does not change the fundamental microenvironment of HRP.

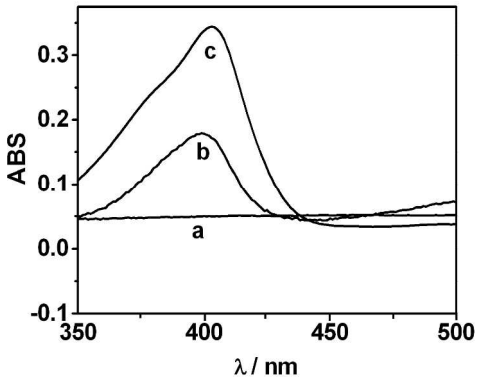

Fig. 3 UV-vis spectra of Au (a), Au-HRP (b) and HRP (c).

Since CD spectroscopy is able to give an insight into the structure and the conformation of the proteins/enzymes,[36] CD spectroscopy is used to further characterize the structural integrity of HRP immobilized on Au. Fig. S2 shows the CD spectra of HRP and Au-HRP, respectively. The CD spectrum of HRP exhibits a negative peak at ca.185 nm (curve a), which is similar to those of the other heme containing proteins.[37] The position of Au-HRP (curve b) is almost the same as that from HRP. The similarities between the CD spectra of curves a and b in Fig. S3 indicate that the structure and the conformation of HRP remain after being immobilized on Au.

3.2. Electrocatalysis of Immobilized HRP to Reduction of H_2O_2

As demonstrated above, Au-HRP composite thin film remains the structure and the conformation of HRP. Because the active HRP can amplify a weak signal and increase detect ability of its target molecule H_2O_2, the electrocatalytic activity of Au-HRP nanocomposite modified electrode toward H_2O_2 is investigated by cyclic voltammograms (CVs). Fig. 4 shows the CVs of

different electrodes in 0.1 M pH 7.0 PBS at 100 mV s^{-1}. Nanoscaled Au modified ITO shows a curve similar to that of ITO. Thus Au is electroinactive in the potential window (Figures not shown). The HRP modified ITO shows a small peak corresponding to the reduction of HRP (curve a′). While the Au-HRP modified ITO exhibits a couple of stable redox peaks which are attributed to the redox of immobilized HRP (curve c′), indicating the presence of Au improves the direct electron transfer between the electrode and the immobilized HRP greatly. The anodic and cathodic peak potentials of the immobilized HRP are at -230 and -310 mV, respectively. The formal potential is -270 mV near the standard electrode potential of -220 mV (vs. SCE) of native HRP in solution,[38] suggesting that most HRP molecules preserve their native structures after the immobilization process. Upon addition of H_2O_2 to the solution, the shape of CV for HRP (curve b′) and Au-HRP (curve d′) both change with increase of reduction currents displaying obvious electrocatalytic behaviors of the free and immobilized HRP to the reduction of H_2O_2, respectively. The electrocatalytic responses are almost similar which shows that the enzyme activity is not affected after the immobilization process. No electrocatalytic current is observable at Au modified ITO when H_2O_2 is added to pH 7.0 PBS (inset).

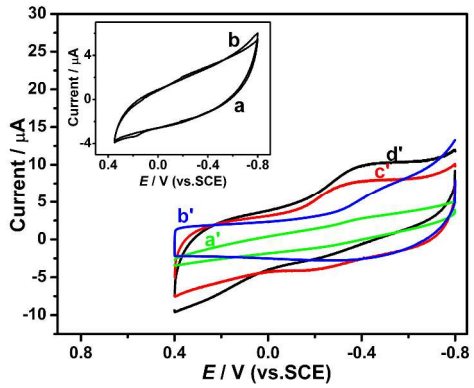

Fig. 4 CVs of HRP/ITO in the absence of H_2O_2 (a′) and in the presence of 0.1 mM H_2O_2 (b′), Au-HRP/ITO in the absence of H_2O_2 (c′) and in the presence of 0.1 mM H_2O_2 (d′) in 0.1 M pH 7.0 PBS at a scan rate of 100 mV s^{-1}. Inset: CVs of Au modified ITO in the absence of H_2O_2 (a) and in the presence of 0.1 mM H_2O_2 (b) at a scan rate of 100 mV s^{-1} in pH 7.0 PBS.

3.3. Optimization Conditions for the Biosensor

Some factors which influenced the performance of the sensor were investigated, including the pH of PBS and the applied potential (Fig. S3). It showed that the current response increased from pH 5.0 to 7.0, and achieved a maximum value at pH 7.0, then decreased from pH 7.0 to 8.0, which was in accordance with the reported for soluble HRP.[39] It meant that the existence of AuNPs did not change the optimal pH value for the bioelectrocatalytic reaction of the immobilized HRP to H_2O_2. In order to obtain maximum sensitivity and bioactivity, PBS with pH of 7.0 was chosen as the buffer. The steady-state reduction current of H_2O_2 increased rapidly as the applied potential moved negatively from -0.2 to -0.4 V, which was due to the increased driving force for the fast reduction of H_2O_2 at lower potential. Then the steady-state current decreased slightly when the applied potential was more negative than -0.4 V. The maximum current occurred at -0.4 V, which was selected as the working potential for amperometric detection of H_2O_2.

3.4. Amperometric Response and Calibration Curve

The amperometric responses of the Au/ITO and Au-HRP/ITO upon successive additions of H_2O_2 to 0.1 M pH 7.0 PBS at an applied potential of -0.4 V were shown in Fig. 5. The Au/ITO showed a much smaller response to H_2O_2 (curve a in Fig. 5) than that of Au-HRP/ITO (curve b in Fig. 5) at the same H_2O_2 concentration. When an aliquot of H_2O_2 was added into the stirring buffer solution, the reduction current rose steeply to reach a stable value. The biosensor achieved the steady state current within 5 s. Such a fast response could be attributed to the following facts: H_2O_2 could diffuse to the enzyme freely since the HRP molecules were exposed to the surface of AuNPs.[39] AuNPs made the HRP molecule immobilize orderly and were favorable to the orientation of the HRP molecules on the electrode surface during the process of electrocatalysis.[40] The linear range of H_2O_2 was from 7.9 μM to 3.6 mM (insert in Fig. 5) with a correlation coefficient of 0.9996 (n=56) which was wider than 8.0 μM to 3.0 mM from HRP on the AuNPs electrodeposited ITO electrode[41] and 12.2 μM to 2.43 mM from HRP on a nano-Au monolayer modified chitosan-entrapped carbon paste electrode (CPE).[42] The detection limit was 0.035 μM at 3σ which was much lower than 2 μM from HRP on the AuNPs electrodeposited ITO electrode[41] and 6.3 μM from HRP on Au monolayer modified chitosan-entrapped CPE.[21] At higher H_2O_2 concentrations, the response followed a typical Michaelis–Menten process. The apparent Michaelis–Menten constant (K_M^{app}), which indicates the enzyme–substrate kinetics, can be obtained from the Lineweaver–Burk equation.[42] It was found to be 0.14 mM, which was smaller than 1.5 mM from H_2O_2 biosensor fabricated by immobilizing HRP on multiwalled carbon nanotubes modified glassy carbon electrode (GCE)[43] and 1.55 mM from H_2O_2 biosensor fabricated by immobilizing HRP on nano-Au with choline covalently modified GCE.[44] It indicated that the prepared Au-HRP modified electrode exhibited a higher affinity for H_2O_2.

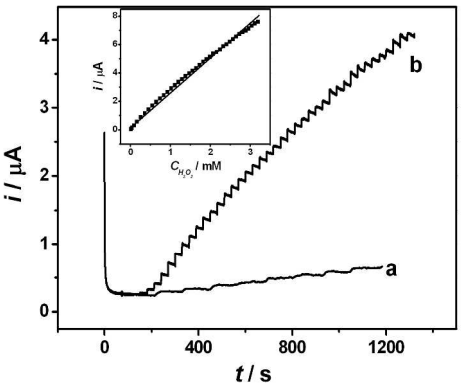

Fig. 5 Current-time response of the Au/ITO (a) and Au-HRP/ITO (b) upon successive additions of H_2O_2 to 0.1 M PBS (pH 7.0) at applied potential of -0.4 V versus SCE. Inset: Calibration plot of peak current versus H_2O_2 concentration.

3.5. Selectivity, Reproducibility and Stability

To evaluate the selectivity of the proposed electrochemical biosensing system, a variety of relevant interfering species including O_2, $OH^{\bullet}$ and $ONOO^-$ in biological system was investigated for control experiments. 5.28%, 6.72% and 4.32% of cathodic current from O_2, $OH^{\bullet}$ and $ONOO^-$ were observed, respectively (Fig. 6). Therefore, the as-prepared electrochemical biosensor would have good selectivity for monitoring of H_2O_2 in biological samples.

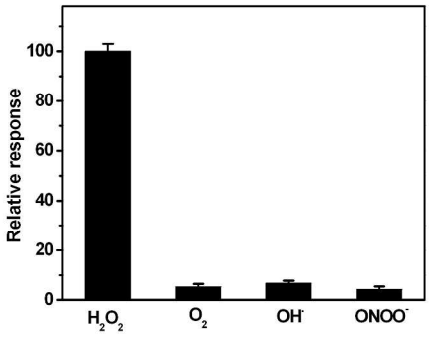

Fig. 6 Effects of common interfering species on the detection of H_2O_2.

The reproducibility of the current response of one enzyme electrode to 0.1 mM H_2O_2 was examined. The relative standard deviation (RSD) was 2.2% for seven successive assays. The electrode to electrode reproducibility was determined from the response to 0.1 mM H_2O_2 at five different enzyme electrodes with RSD of 3.6%. The good reproducibility may be due to the fact that the AuNPs made HRP molecules chemisorbed orderly and attach firmly onto the surface of AuNPs.

The long-time stability of the enzyme electrode was investigated over a 30-day period. When the biosensor was stored in the refrigerator at 4 °C and measured every 10 days, no obvious change was found in the response to 0.1 mM H_2O_2. The good long-term stability could be attributed to the fact that there were strong interactions between HRP molecules and the surface of AuNPs, thus, HRP molecules could be firmly immobilized on the surface of the Au and made the enzyme electrode stable.

3.6. Monitoring the H_2O_2 Released from Raw 264.7 Cells

As mentioned above, the sensor exhibited a good sensitivity, selectivity, stability and reproducibility which were provided to be used in in-vitro determination of H_2O_2 released from living cells. Fig. 7 showed the electrochemical response obtained at Au-HRP modified ITO surface and towards rat 264.7 macrophage cells adhered on the electrode surface at the applied potential of -0.4 V in the absence (A) and presence (B) of phorbol-12-myristate-13-acetate (PMA), which was reported to generate H_2O_2 from cells.[45] A much higher increased cathodic current was observed after the addition of PMA. The increased response was attributed to the reduction of H_2O_2 released from living cells. Thus, the sensor can monitor the H_2O_2 released from the cells. This result is consistent with the detecting of H_2O_2 in PMA-treated macrophages by other reports.[46-48]

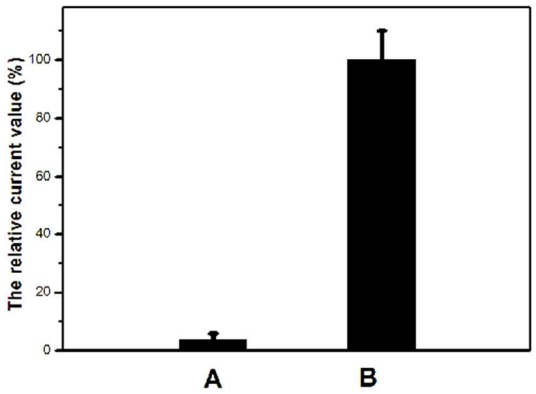

Fig. 7 Electrochemical responses of Au-HRP modified electrode toward raw 264.7 at an applied potential of -0.4 V in the absence (A) and presence (B) of 10 mM PMA.

4. Conclusions

In summary, a novel method for immobilizing biomolecules on the surface of the electrode has been introduced. HRP has been successfully chemisorbed onto AuNPs that formed in liquid-liquid interface via the interactions between AuNPs and HRP. The AuNPs provided the necessary conduction pathway and efficient electron tunneling. Furthermore, such modified HRP electrodes exhibited good electrocatalysis towards the reduction of H_2O_2. The resulting biosensor exhibited fast amperometric response, low detection limit, wide linear range to H_2O_2, high sensitivity, good reproducibility, and long-term stability. This approach provided a novel and simple method for developing the immobilization method and a new class of electrochemical biosensor for H_2O_2. More interestingly, it could be successfully exploited for the determination of H_2O_2 released from living cells which was expected to have the potential application in cellular biology.

Acknowledgements

This research was financially supported by the National Natural Science Foundation of China for the project (Nos. 21475062, 21175069, 21171096 and 21271105), Foundation of the Jiangsu Education Committee (11KJA150003), and Research Fund for the Doctoral Program of Higher Education of China (20113207110005). We appreciate the financial support from the Priority Academic Program Development of Jiangsu Higher Education Institutions and the Program for Outstanding Innovation Research Team of Universities in Jiangsu Province.

Notes and references

1 D. W. Kimmel, G. LeBlanc, M. E. Meschievitz and D. E. E. Cliffel, *Anal. Chem.,* 2012, **84**, 685-707.
2 S. K. Arya and S. Bhansali, *Chem. Rev.,* 2011, **111**, 6783-6809.
3 S. J. Bao, C. M. Li, J. F. Zang, X. Q. Cui, Y. Qiao and J. Guo, *Adv. Funct. Mater.,* 2008, **18**, 591-599.
4 R. Dronov, D. G. Kurth, H. Möhwald, R. Spricigo, S. Leimkühler, U. Wollenberger, K. V. Rajagopalan, F. W. Scheller and F. Lisdat, *J. Am. Chem. Soc.,* 2008, **130**, 1122-1123.
5 C. Zhao, K. G. Qu, Y. J. Song, J. S. Ren and X. G. Qu, *Adv. Funct. Mater.,* 2011, **21**, 583-590.
6 M. Tasso, S. L. Conlan, A. S. Clare and C. Werner, *Adv. Funct. Mater.,* 2012, **22**, 39-47.
7 F. Z. Kong and Y. F. Hu, *Anal. Bioanal. Chem.,* 2012, **403**, 7-13.
8 Z. Qu, S. Muthukrishnan, M. K. Urlam, C. A. Haller, S. W. Jordan, V. A. Kumar, U. M. Marzec, Y. Elkasabi, J. Lahann, S. R. Hanson and E. L. Chaikof, *Adv. Funct. Mater.,* 2011, **21**, 4736-4743.
9 H. Tang, F. Yan, P. Lin, J. B. Xu and H. L. W. Chan, *Adv. Funct. Mater.,* 2011, **21**, 2264-2272.
10 Q. Zeng, J. S. Cheng, L. H. Tang, X. F. Liu, Y. Z. Liu, J. H. Li and J. H. Jiang, *Adv. Funct. Mater.,* 2010, **20**, 3366-3372.
11 C. J. Doonan, H. L. Wilson, K. V. Rajagopalan, R. M. Garrett, B. Bennett, R. C. Prince and G. N. George, *J. Am. Chem. Soc.,* 2008, **130**, 6298-6298.
12 J. Yang, R. Rothery, J. Sempombe, J. H. Weiner and M. L. Kirk, *J. Am. Chem. Soc.,* 2009, **131**, 15612-15614.
13 A. V. Astashkin, K. Johnson-Winters, E. L. Klein, C. J. Feng, H. L. Wilson, K. V. Rajagopalan, A. M. Raitsimring and J. H. Enemark, *J. Am. Chem. Soc.,* 2008, **130**, 8471-8480.
14 K. Wang, T. X. Wei, W. W. Tu, M.Han and Z. H. Dai, *Anal. Methods,* 2013, **5**, 1909-1914.
15 X. Wang, Q. Peng and Y. Li, *Acc. Chem. Res.,* 2007, **40**, 635-643.
16 C. N. R. Rao and K. P. Kalyanikutty, *Acc. Chem. Res.,* 2008, **41**, 489-499.
17 K. Wang, T. X. Wei, W. W. Tu, M. Han and Z. H. Dai, *Anal. Methods*, 2013, **5**, 1909-1914.
18 J. S. Ellis, J. Strutwolf and D. W. M. Arrigan, *Phy. Chem. Chem. Phy.,* 2012, **14**, 2494-2500.
19 M. H. Lin, H. Pei, F. Yang, C. H. Fan and X. L. Zuo, *Adv. Mater.,* 2013, **25**, 3490-3496.
20 Y. Liu and P. Y. Wu, *ACS Appl. Mater. Interfaces,* 2013, **5**, 5832-5844.
21 S. X. Mao, Y. M. Long, W. F. Li, Y. F. Tu and A. P. Deng, *Biosens. Bioelectron.,* 2013, **48**, 258-262.
22 H. J. Wang, R. Yuan, Y. Q. Chai, Y. L. Cao, X. X. Gan, Y. F. Chen and Y. Wang, *Biosens. Bioelectron.,* 2013, **43**, 63-68.
23 R. Akter, M. A. Rahman and C. K. Rhee, *Anal. Chem.,* 2012, **84**, 15, 6407-6415.
24 A. K. M. Kafi and M. J. Crossley, *Biosens. Bioelectron.,* 2013, **42**, 273-279.
25 G. N. Li, T. T. Li, Y. Deng, Y. Cheng, F. Shi, W. Sun and Z. F. Sun, *J. Solid State Electrochem.,* 2013, **17**, 2333-2340.
26 M. H. Freeman, J. R. Hall and M. C. Leopold, *Anal. Chem.,* 2013, **85**, 4057-4065.
27 A. A. Saei, P. Najafi-Marandi, A. Abhari, M. de la Guardia and J. E. N. Dolatabadi, *Trac-Trends in Anal Chem.,* 2013, **42**, 216-227.
28 L. Wang, W. Wen, H. Y. Xiong, X. H. Zhang, H. S. Gu and S. F. Wang, *Anal. Chim. Acta,* 2013, **758**, 66-71.
29 J. W. Di, S. H. Peng, C. P. Shen, Y. S. Gao and Y. F. Tu, *Biosens. Bioelectron.,* 2007, **23**, 88-94.
30 R. R. D. Moreira, I. Z. Carlos and W. Vilegas, *Biol. Pharm. Bull.,* 2001, **24**, 201-204.
31 V. Darley-Usmar, H. Wiseman and B. Halliwell, *FEBS Lett.,* 1995, **369**, 131-135.
32 D. Salvemini, H. Ischiropoulos and S. Cuzzocrea, *Methods Mol. Biol.,* 2003, **225**, 291-303.
33 A. M. Niess, H. H. Dickhuth, H. Northoff and E. Fehrenbach, *Exerc. Immunol. Rev.,* 1999, **5**, 22-56.
34 J. J. Haddad, *Cell. Signal.,* 2002, **14**, 879-897.
35 T. J. Guzik, R. Korbut and T. Adamer-Guzik, *J. Physiol. Pharmacol.,* 2003, **54**, 469-487.
36 F. Ballester, G. Solaini and G. Lenaz, J. *Biochem.,* 1987, **241**, 285-290.
37 M. R. Hanlon, R. R. Begum, R. J. Newbold, D. Whitford and B. A. Wallace, J. *Biochem.,* 2000, **352**, 117-124.
38 H. A. Harbury, J. *Biol. Chem.,* 1957, **225**, 1009-1024.
39 Y. Xiao, H. X. Ju and H. Y. Chen, *Anal. Biochem.,* 2000, **278**, 22-28.
40 J. G. Zhao, R. W. Henkens, J. Stonehuerner, J. P. O'Daly and A. L. Crumbliss, *J. Electroanal. Chem.,* 1992, **327**, 109-119.
41 T. Kida, *Langmuir,* 2008, **24**, 7648-7650.
42 R. A. Kamin and G. S. Wilson, *Anal. Chem.,* 1980, **52**, 1198-1205.
43 Y. Y. Peng, A. K. Upadhyay and S. M. Chen, *Electroanalysis,* 2010, **22**, 463-470.
44 Y. Zheng, X. Q. Lin and J. Chin, *Anal. Chem.,* 2008, **36**, 604-608.
45 Q. Y. Lin, L. J. Jin, Z. H. Cao, Y. N. Lu, H. Y. Xue and Y. P. Xu, *Phytother. Res.,* 2008, **22**, 740-745.
46 B. C. Dickinson, C. Huynh and C. J. Chang, *J. Am. Chem. Soc.*, 2010, **132**, 5906-5915.
47 M. Abo, Y. Urano, K. Hanaoka, T. Terai, T. Komatsu and T. Nagano, *J. Am. Chem. Soc*., 2011, **133**, 10629-10637.
48 W. K. Oh, Y. S. Jeong, S. Kim and J. Jang, *ACS Nano*, 2012, **6**, 8516-8524.